Single germanium vacancy centers in nanodiamonds with bulk-like spectral stability

Cite as: AVS Quantum Sci. 3, 012001 (2021); https://doi.org/10.1116/5.0035937
Submitted: 03 November 2020 . Accepted: 15 December 2020 . Published Online: 29 January 2021

M. Nahra, D. Alshamaa, R. Deturche, V. Davydov, L. Kulikova, V. Agafonov, and C. Couteau

AVS Quantum Science ARTICLE scitation.org/journal/aqs

Single germanium vacancy centers in nanodiamonds with bulk-like spectral stability

Cite as: AVS Quantum Sci. 3, 012001 (2021); doi: 10.1116/5.0035937
Submitted: 3 November 2020 · Accepted: 15 December 2020 ·
Published Online: 29 January 2021

M. Nahra,[1] D. Alshamaa,[2] R. Deturche,[1] V. Davydov,[3] L. Kulikova,[3] V. Agafonov,[4] and C. Couteau[1,a)]

AFFILIATIONS

[1]Laboratory Light, Nanomaterials and Nanotechnologies (L2n), CNRS ERL 7004, University of Technology of Troyes, 12 rue Marie Curie, 10004 Troyes Cedex, France
[2]Laboratory of Informatics, Robotics and Microelectronics of Montpellier (LIRMM), UMR 5506, University of Montpellier–CNRS, 34095 Montpellier Cedex, France
[3]L.F. Vereshchagin Institute for High Pressure Physics, Russian Academy of Sciences, Troitsk, Moscow 142190, Russia
[4]GREMAN, UMR CNRS CEA 7347, Université de Tours, 37200 Tours, France

[a)]Electronic mail: christophe.couteau@utt.fr

ABSTRACT

Motivated by the success of group IV color centers in nanodiamonds (NDs) for hybrid technology requiring a single photon source, the authors study single germanium-vacancy (GeV^-) centers in NDs at room temperature with size ranging from 10 to 50 nm and with remarkable spectral properties. The authors characterize their zero-phonon line, study their internal population dynamics, and compare their emission properties in the framework of a three level model with intensity dependent de-shelving. Furthermore, the authors characterize their lifetime, polarization, and brightness. The authors find a maximum photon emission count rate of 1.6 MHz at saturation. The authors also report a polarization visibility of 92% from the fluorescence light, which potentially makes GeV^- centers good candidates for quantum key distribution requiring polarized single photons. The authors show that GeV^- centers in NDs presented in this work have a comparable spectral stability compared to their bulk counterpart, which is needed for future applications using nanodiamonds.

Published by the AVS. https://doi.org/10.1116/5.0035937

I. INTRODUCTION

Single defect centers in diamond have become a highly attractive candidate for solid-state single photon source applications.[1–3] Nowadays, many studies are being carried out on nitrogen vacancy (NV^-) and silicon vacancy (SiV^-) color centers showing some limitations. Despite the remarkable electronic spin coherence of NV^- centers,[4] they suffer from a low optical emission of only 4% into the zero-phonon line (ZPL), as well as a polar symmetry rendering it sensitive to external perturbations.[5] In contrast, SiV^- centers offer exceptional optical properties with a narrow linewidth, 80% of the emission concentrated in the ZPL and a small phonon side band (PSB).[6] More importantly, the SiV^- inversion symmetry is responsible for low emission into the PSB and makes it robust against external perturbations such as fluctuating electric and magnetic fields. However, the energy level of SiV^- can be significantly altered in the presence of strong crystal strain.[7] In addition, it suffers from low quantum efficiency[8,9] and low coherence time[10] due to nonradiative processes owing to phonon-mediated transitions.[11] These limiting nonradiative processes are overcome at mK temperatures[12] or in the presence of strain.[13] Moreover, color centers in bulk diamond suffer from low collection efficiency due to the high refractive index of diamond.[14–16] Diamond nanostructures can overcome this issue. In particular, small nanodiamonds (NDs) have reduced light scattering, and they can be more easily coupled to photonic structures, which makes them more appropriate for hybrid technologies.[17–19] However, color centers in NDs present a large spectral distribution of their ZPL, which is a major drawback for such emitters. Strain and charge fluctuations at the surface of small NDs are responsible for this random spectral distribution.[20–23]

To overcome these issues, research has been oriented toward a more efficient and bright color center in small NDs, the GeV^- center.[24] This defect is a promising color center with superior optical properties. It possesses the same inversion symmetry as the SiV^- color center,[25,26] thus having equivalent optical properties.[27] However, it outperforms the SiV^- color center with its higher quantum efficiency.[24] We point out here that recently another group IV color centers namely tin-vacancy (SnV)[28,29] and lead-vacancy (PbV)[30,31] have received attention. They have shown equivalent optical properties along with a better coherence time than that of the SiV color center.[28]

In this article, we study single GeV^- centers in NDs with a mean size of about 20 nm, grown using the high-pressure-high-temperature (HPHT) method. First, we analyze their ZPL properties, showing a stable ZPL with a small spectral shift as compared to their bulk counterpart. We then demonstrate the single photon nature of the emitted light from single NDs using a Hanbury, Brown, and Twiss setup. Then, in order to better understand the emission properties, we proceed by studying the internal population dynamics of two typical single GeV^- centers from two distinct NDs. Our study is analyzed within the framework of an extended three level system model with intensity dependent de-shelving.[8] Finally, we characterize their full optical properties such as brightness, lifetime, and polarization.

II. METHODS

We studied several GeV^- centers in diamond nanocrystals produced using the HPHT technique. To form a complex GeV^- center, tetraphenylgermanium ($C_{24}H_{20}Ge$) was introduced during the growth process and incorporated into diamond nanocrystals. After that, and in order to remove the excess of Ge and germanium oxide (GeO_2), NDs were suspended in hydrofluoric acid (HF) at 160 °C for 2 h. Later on, they were dissolved in a solution of ultrapure water and isopropanol. Next, they were ultrasonicated to disperse the nanodiamonds and finally spin coated on a silicon substrate cleaned prior to deposition. See the supplementary material for the detailed growth technique.[45] Figure 1(a) shows a transmission electron microscopy (TEM) image of some GeV^- centers in NDs of different sizes ranging from 10 to 50 nm, with an average of 20 nm taken after the chemical and ultrasonic treatment. In order to investigate the optical properties of the GeV^- centers in NDs and identify whether a center is single or not, the sample was characterized by optical micro-photoluminescence (PL) at room temperature. See the supplementary material for the experimental setup used for optical characterization.[45] The GeV^- centers were excited using an off-resonantly continuous wave laser at 532 nm. The laser light was focused through a 100× dry microscope objective, and the fluorescence was collected using the same objective. The collected fluorescence light was filtered by a narrow band-pass with a full-width at half maximum (FWHM) of 14 nm around 600 nm in order to avoid the Raman signal of diamond and other background emission from the substrate and the carbon matrix of the NDs. After that, it was directed to one of the two paths: a spectrometer for photoluminescence measurements or a Hanbury, Brown, and Twiss setup for the second order correlation function ($g^{(2)}(\tau)$). For the purpose of polarization measurement, a linear polarizer was added to the detection path and rotated from 0° to 360°.

III. RESULTS AND DISCUSSION

A. Photoluminescence spectra

In order to study the optical properties of our GeV^- color centers, we first performed PL measurements at room temperature. Figure 1(b) shows normalized PL spectra for two single GeV^- centers with a ZPL centered at 605.5 and 601.5 nm, respectively. Using a Lorentzian fit of the ZPL, we measure a FWHM of 4.5 nm for GeV1. However, for GeV2, we use a multi-peak Lorentzian fit and measure a FWHM of 5.5 nm for the ZPL. This is comparable with the observations of a FWHM of 5.5 nm in bulk diamond at room temperature.[27] We note that the FWHM around 5 nm is supposed to be caused by the isotopic shift of the ZPL due to the presence of Ge isotopes.[27,32] Moreover, we measure the Huang Rhys factor S defined by $I_{ZPL}/I_{tot} = e^{-S}$ in order to determine the strength of the electron–phonon coupling.[33] A value of the S factor equal to zero corresponds to a pure emission into the ZPL without phonon coupling, while a value higher than one implies a strong electron–phonon coupling. This is typically the case for NV^- centers with $S = 3.73$.[34] In our case, we obtained S factors of 0.5 and 0.79 for GeV1 and GeV2, respectively. These values are lower than other values reported for GeV of 1.3.[35] These measurements were carried out on 20 centers. It was found that these centers exhibit almost the same ZPL, with a slight variation of ±2 nm around 603.5 nm. It was also found that the FWHM varies from 4 and 7 nm. In addition, an average S factor of $S_{mean} = 0.65$ was reported. Figure 1(c) presents the distribution of the ZPL, FWHM, and S factor for 20 studied centers, which allowed us to come up with the mean values of 603.5 nm, 5.2 nm, and 0.65, respectively. The distribution around the mean or the standard deviation was calculated and found to be 1.11, 1.18, and 0.08 for the ZPL, FWHM, and S factor, respectively. Since there are a very few studies on GeV^- centers in NDs, we compare the stability of ZPL to that of SiV^- in NDs. Previous studies reported a wide spread of the position of the ZPL of SiV in NDs.[20,23] This is attributed to the strain effect within the NDs. Other studies demonstrated that an improved crystalline quality can be obtained via bead assisted sonic disintegration of a polycrystalline chemical vapor deposition film.[36] Also, a special surface treatment of NDs with hydrogen-plasma[37] or oxygen[21] improves the spectral stability of the SiV^- ZPL. It is worth mentioning that no additional surface treatment after the acid treatment was performed on our NDs.

The narrow distribution of the ZPL position in the PL spectra of GeV^- centers in the studied NDs indicates low inhomogeneous broadening and low spectral diffusion. On one hand, the low inhomogeneous distribution is due to the low internal strain of NDs obtained on the basis of hydrocarbon growth systems in the (P, T) region of the thermodynamic stability of diamond at a pressure of 8.0 GPa and at rather high temperatures of ≈ 1500 °C. This facilitates the efficient annealing of structural defects in diamond, leading to low strain NDs. On the other hand, the low spectral diffusion is, in our opinion, due to the reduction of the number of electroactive surface defects. This is probably the fluorination of the surface of nanodiamonds during their preliminary chemical treatment according to the following chemical reaction: Diam-OH + HF → Diam-F + H_2O. These properties render our GeV^- centers potentially suitable for quantum technologies as they have the potential to provide indistinguishable single photons.

B. Second order correlation function $g^{(2)}$

In order to investigate the presence of single photons emitted by a single GeV^- center and to understand its internal population dynamics, we measured the intensity autocorrelation function $g^{(2)}$ of some of our single defect centers. An example of a $g^{(2)}$ result under a pulsed and continuous laser excitation is shown in Fig. 2. The obtained value of $g^{(2)} = 0.2$ at $\tau = 0$ ns is a clear evidence of a single photon source from the GeV^- defect emission. In the following, we aim to study the internal population dynamics of our GeV^- centers using a continuous laser at various excitation powers. To this end, we considered seven GeV^- centers in distinct NDs and measured their intensity correlation function $g^{(2)}$. Six of the seven studied GeV centers have presented almost identical properties. We made the choice to show in this article the results of one of these six typical GeV^- centers, namely,

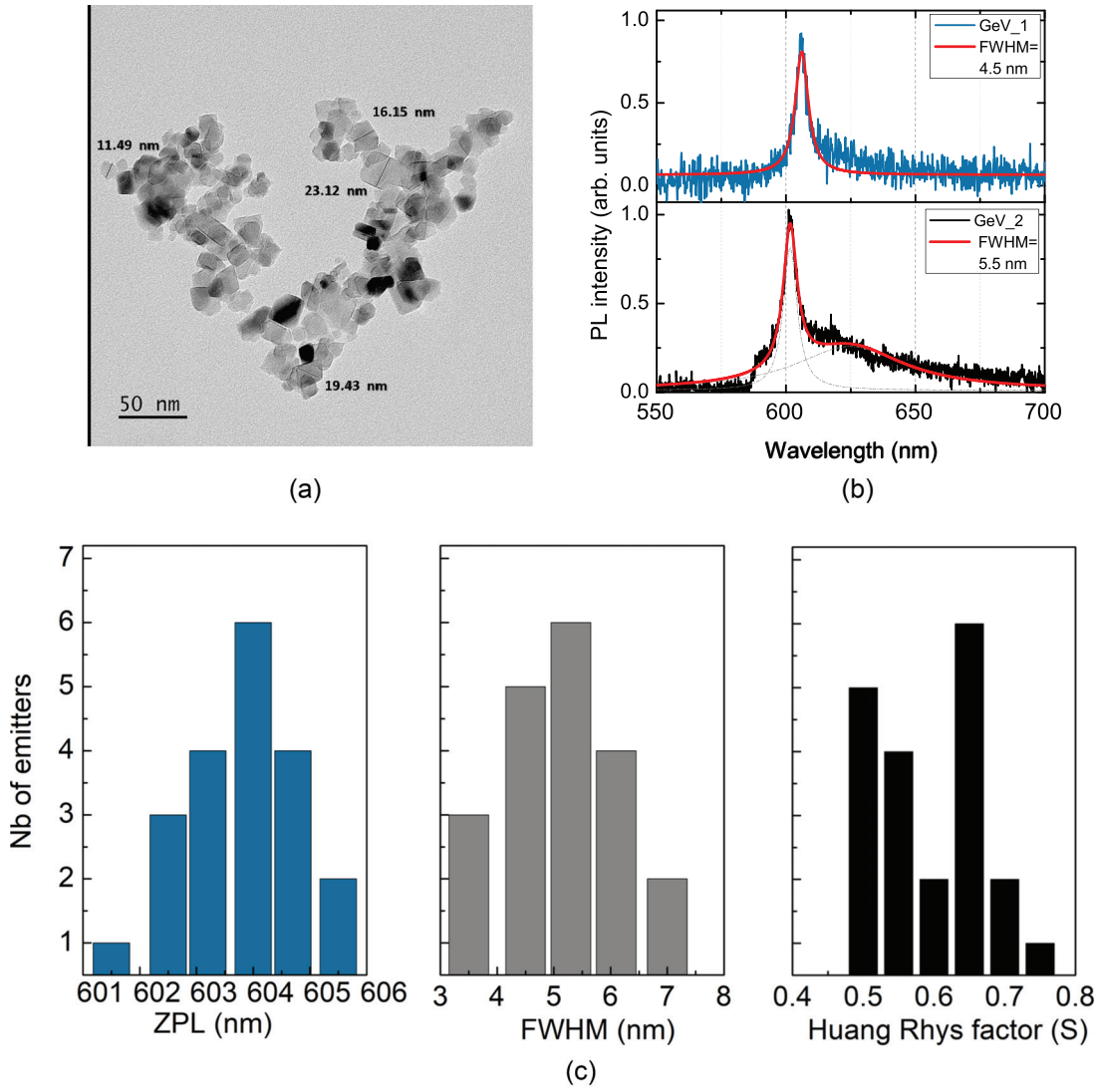

FIG. 1. Characterization of single GeV centers. (a) TEM image for HPHT nanodiamonds taken after ultrasonic treatment. Their size average is 20 nm. (b) Photoluminescence (PL) spectrum for two GeV centers. The red line denotes a Lorentzian fit of the ZPL for GeV1, while it denotes a multi-peak Lorentzian fit of both the ZPL and PSB for GeV2. (c) Histogram distributions of ZPL, FWHM, and Huang Rhys factor for 20 emitters.

GeV1. We also present results from the seventh GeV$^-$ center, namely, GeV2, which we studied more thoroughly as its properties were different from the other six ones as we will show. Figures 4(a) and 4(b) present normalized $g^{(2)}$ functions measured at different excitation powers. The $g^{(2)}$ function does not follow a Poissonian source over all the delay time. Rather, at intermediate delay, the $g^{(2)}$ function increases and then decreases to a constant value and becomes approximately flat for a very long delay time, where $g^{(2)}(\tau \to \infty) = \text{constant}$. Thus, the $g^{(2)}$ function is normalized to $g^{(2)}(\tau) = 1$ for these regions. The pronounced photon antibunching at zero time delay clearly proves the single photon nature of the light emitted by these two GeV centers under investigation. We point out here that the data of $g^{(2)}$ are given without any correction factor from background emission. As one could expect, for longer time delays, a photon bunching can be noticed where the value of $g^{(2)}$ exceeds one. The presence of bunching and antibunching allows us to represent the GeV$^-$ color center emission by a three level model comprising a ground state (1), an excited state (2), and a metastable state (3). The $g^{(2)}$ function for an ideal three level system can be expressed as follows:

$$g^{(2)}(\tau) = 1 - (1 + a)e^{(-|\tau|/\tau_1)} + ae^{(-|\tau|/\tau_2)}, \quad (1)$$

where τ_1 and τ_2 designate the antibunching and bunching time constants, respectively, with a the so-called degree of bunching. The details of the employed $g^{(2)}$ function can be found here.[38] This typical function reflects the population dynamics of state 2. The parameters a, τ_1, and τ_2 can be obtained via solving the rate equations for the populations in the system,[39] as shown in the following set of equations:

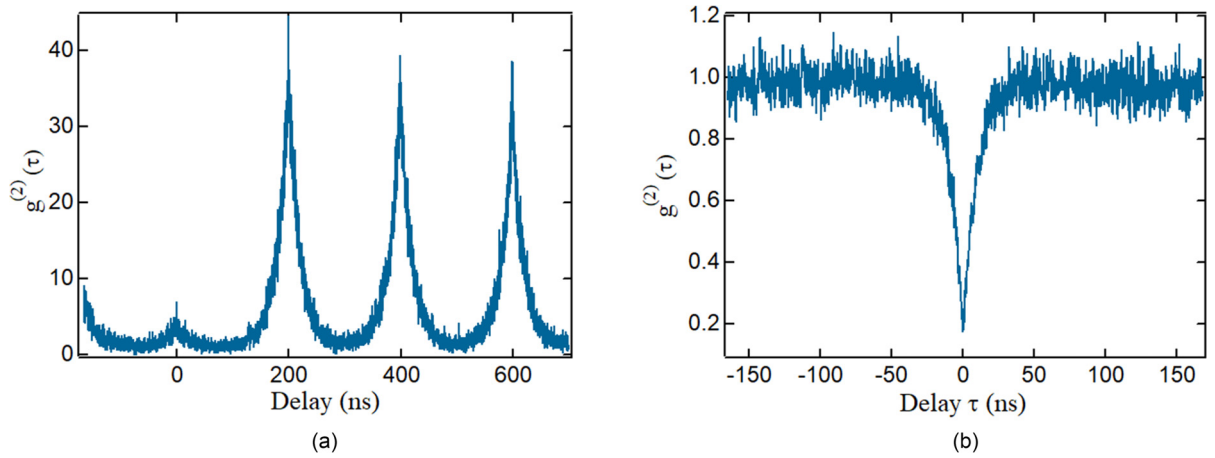

Fig. 2. Second order correlation function for GeV2: (a) with a pulsed excitation laser and (b) with a continuous excitation laser. A value of less than 0.5 is a clear evidence for the single photon nature of the emitted luminescence.

$$\tau_{1,2} = \frac{2}{A \pm \sqrt{A^2 - 4B}}, \tag{2}$$

$$A = k_{12} + k_{21} + k_{23} + k_{31}, \tag{3}$$

$$B = k_{12}k_{23} + k_{12}k_{31} + k_{21}k_{31} + k_{23}k_{31}, \tag{4}$$

$$a = \frac{1 - \tau_2 k_{31}}{k_{31}(\tau_2 - \tau_1)}, \tag{5}$$

where k_{ij}, $i, j \in \{1, 2, 3\}$ represent the rate coefficients from state i to state j. After replacing A and B in Eq. (2) by their expressions in Eqs. (3) and (4) and simplifying, the time constant τ_2 can be expressed as $\tau_2 = 1/k_{31}$. In this model, all the rate coefficients are intensity-independent except the pumping rate $k_{12} = KP$, which depends linearly on the excitation power. However, when we consider k_{31} to be constant, the model fails to fit our experimental data. As Figs. 4(c) and 4(d) show, τ_2 is intensity dependent, which means that k_{31} should not be constant.

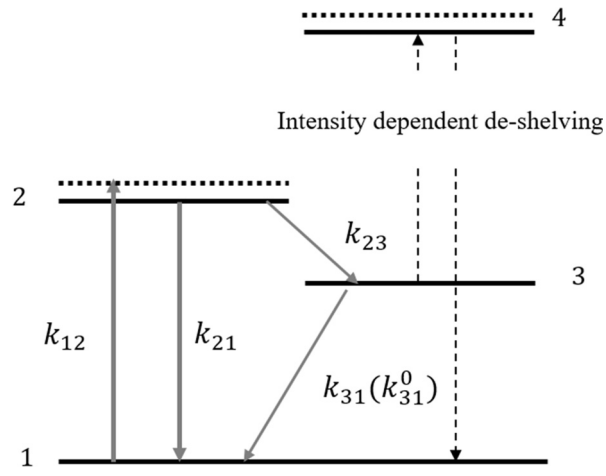

Fig. 3. Three level system with intensity dependent de-shelving used to study the population dynamics of GeV^- color centers in this article.

For that reason, we extend our model to a three level system comprising an intensity dependent de-shelving state. Figure 3 illustrates the three level system model with intensity dependent de-shelving. Here, k_{31} follows a saturation law as shown by the following equation:

$$k_{31} = \frac{A_1 P}{P + B_1} + C_1, \tag{6}$$

where $A_1 = k_{31}^{\infty} = 1/\tau_2^{\infty}$ and $C_1 = k_{31}^0 = 1/\tau_2^0$ represent the high and low power limits of the de-shelving process, respectively, and B_1 represents the saturation power of the de-shelving state. A similar model with intensity dependent de-shelving was used in the past for single molecules,[40] NE8 centers,[41] and SiV color centers.[8] In order to determine the model parameters A_1, B_1, C_1, K, and k_{21} and k_{23}, an optimization algorithm was developed to fit the model to the experimental data at a given excitation power. The same obtained parameters were employed in our model to fit the experimental data at all excitation powers. Table I summarizes the obtained fitting parameters for the two studied GeVs. See the supplementary material for the average and standard deviation of the parameters of the six similar GeVs.[45] Also, see the supplementary material for details of the optimization algorithm and the calculation of the parameters.[45]

Figures 4(c) and 4(d) show the experimental and fitting data of the variation of the parameters a, τ_1, and τ_2 as a function of the excitation power. The value of a for GeV2 reaches 2 and is higher than that for GeV1, which is less than 1. This means that GeV2 has a stronger coupling to the metastable state than GeV1. As mentioned earlier, this behavior for GeV2 was found to be different from that for the other

Table I. Optimized fitting parameters deduced using the extended three level model. All parameters A_1, C_1, k_{21}, and k_{23} are expressed in GHz, while B_1 is expressed in mW.

	A_1 (GHz)	B_1 (mW)	C_1 (GHz)	k_{21} (GHz)	k_{23} (GHz)
GeV1	0.0051	0.45	0.0022	0.1014	0.0065
GeV2	0.002	1.42	0.0007	0.0458	0.0052

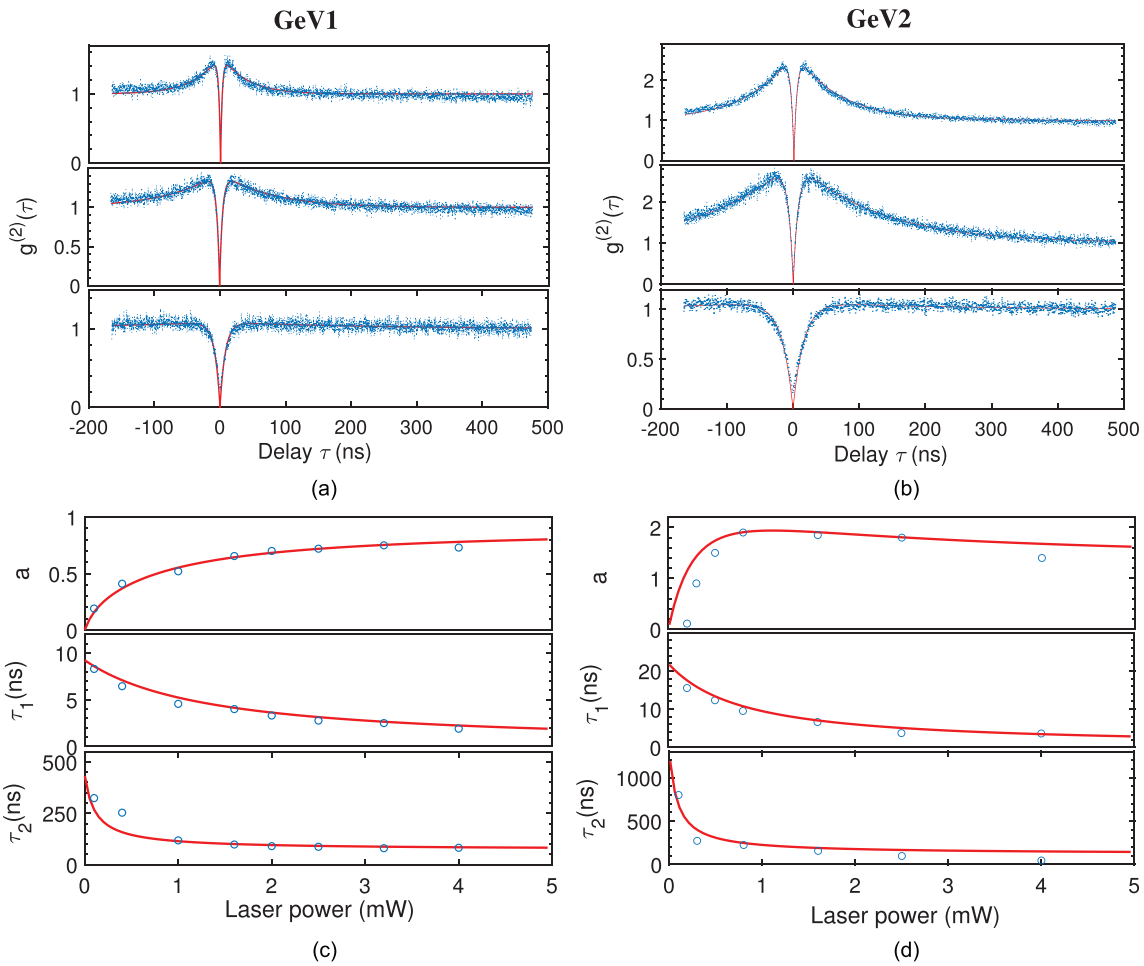

FIG. 4. $g^{(2)}$ modeling according to a three level system with intensity dependent de-shelving. (a) and (b) Three representative normalized autocorrelation curves taken at different excitation laser powers of 0.1, 1, and 4 mW for GeV1 and GeV2, respectively. (c) and (d) Power dependence of the fitting parameters a, τ_1, and τ_2 for GeV1 and GeV2, respectively.

6 GeV$^-$ centers studied (including GeV1). The value of the ratio k_{23}/k_{31} gives us the probability of transition to the metastable state, which is lower for GeV1. Beyond the saturation, and for $P \rightarrow \infty$, we noticed a ratio of k_{23}/A_1 equal to 1.1 for GeV1 lower than that of GeV2 equal to 2.6. This result is in agreement with the higher degree of bunching a obtained for GeV2 as shown in Figs. 4(c) and 4(d). The difference in the coupling to the metastable state, which, in turn, affects the brightness of GeV$^-$, might be due to a different concentration of the nitrogen donor in each ND. The suggested mechanism at play is a change in the charge state of the emitter between the $(-)$ and $(2-)$ states, as mentioned in Ref. 42. Our choice of these two GeVs is based on the significant difference in terms of their population dynamics. These, in turn, affect the optical properties of the GeV$^-$ centers such as saturation and lifetime, as will be discussed in detail in Secs. III C and III D.

C. Fluorescence decay rate

The rate coefficient analysis allows us to estimate both the excited and metastable state lifetimes, expressed by $\tau_1 = 1/k_{21}^0$ and $\tau_2 = 1/k_{31}^0$, respectively. To validate the value of τ_1 obtained by the model, we compare it to the experimental data obtained by a direct measurement of the lifetime using a pulsed laser. Figure 5(b) shows a lifetime measurement under a 532 nm pulsed laser excitation at a repetition rate of 10 MHz. To validate the fluorescence decay of these emitters, the data were fitted using a single exponential model according to the equation $I = I_0 + Ae^{(-t/|\tau|)}$. After normalization, the model is simplified to $I = e^{(-t/|\tau|)}$. Using the fitted model, a total excited state lifetime of 10.11 ns and 20.5 ns for GeV1 and GeV2, respectively, was found. These values match the calculated excited state lifetime using the three level model according to $\Gamma^{-1} = (k_{21} + k_{23})^{-1}$, where the values of 9.25 ns and 19.58 ns were calculated for GeV1 and GeV2, respectively. The direct measurement of the lifetime reflects the total decay rate of the color center from its excited state. It includes the radiative and nonradiative decay paths $\Gamma = \Gamma_{rad} + \gamma_{nr}$. We point out that the shorter lifetime for GeV1 comes along with an increase in its brightness, which will be shown in Sec. III D.

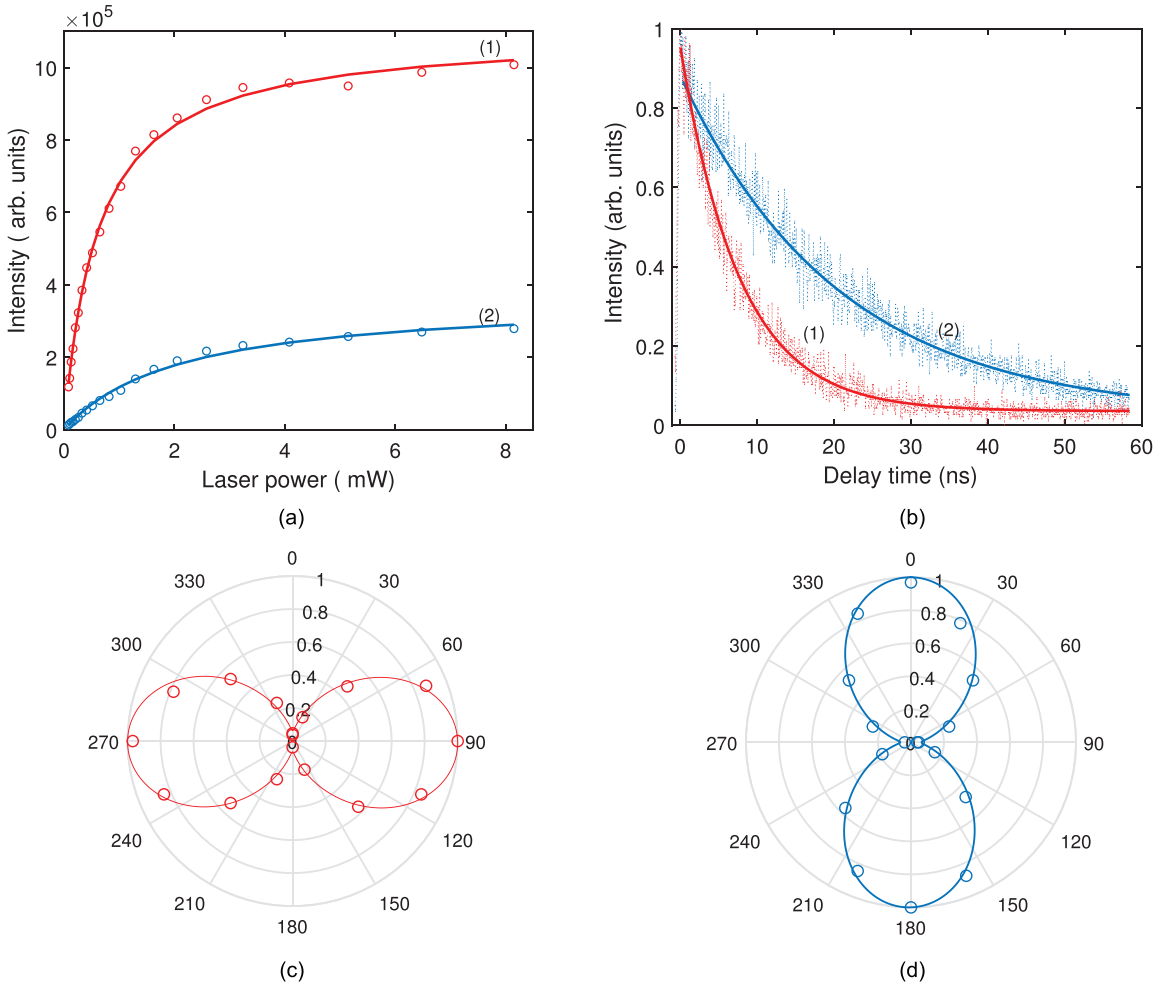

FIG. 5. Optical properties of single GeV$^-$ centers. (a) Saturation curves taken for GeV1 and GeV2 centers show different brightness between emitters with background subtraction. (b) Lifetime measurement under a green pulsed laser for GeV1 and GeV2. (c) and (d) Emission polarization measurements for GeV1 and GeV2. All solid lines refer to the fitting model (see the main text).

D. Brightness of single GeV$^-$ centers

The brightness of the emitters is a very important figure of merit for a single photon source. Figure 5(a) displays the saturation curves of the two single color centers GeV1 and GeV2 taken after background correction. The solid fitted curves follow the equation $I = I_\infty(P/P_{\text{sat}} + P)$, where I_∞ is the maximum emission intensity and P_{sat} is the saturation power. Using the fitting curves, we measure a maximum emission intensity of 1.5 MHz and 0.2 MHz for GeV1 and GeV2, respectively, with a saturation power of 0.56 and 1.5 mW. The average I_∞ measured for the six other GeVs gives a value of 0.856 MHz. This indicates a 10-fold enhancement in the brightness of GeV$^-$ centers than that in bulk diamond reported elsewhere.[26] This enhancement is expected to be due to the very small size of our NDs. Indeed, the small size of the NDs results in an efficient suppression of total internal reflection, thus enabling us to collect more photons with the microscope objective.[43] We point out here that these saturation curves are done on the ZPL with a narrow band-pass filter with a FWHM of 14 nm around 600 nm. We, thus, expect that this value will increase if a wider band-pass is used. Moreover, our dry microscope objective has an NA = 0.95 and will, thus, not collect as much as an oil-immersion objective would, and therefore, higher count rates are expected. Additional loss is due to the dichroic mirror used in our PL setup that suffers from a polarization-dependent loss of the emitted light. Therefore, it appears that the GeV$^-$ centers studied in this article have a higher quantum yield than SiV$^-$ in general, which has a similar saturation fluorescence but a lower excited state lifetime of less than 1 ns.[14] GeV1 showed a stable emission during 15 min, even at a very high excitation power. While most of the GeV$^-$ centers presented a stable emission, few others such as GeV2 have shown an unstable emission. This is due to the high coupling to the metastable state where the emitter goes in a "dark" or an "OFF" state. This is in agreement with the high value of a obtained using our proposed model.

E. Polarization of single GeV$^-$ centers

In this paragraph, we investigate whether these single GeV defects act as single dipole emitters. To this end, we check the polarization sensitivity by rotating a polarizer in the detection path. To verify that the emission is not due to a scattering from a substrate, we excite some position on the substrate without NDs using the same filter to remove the background from the fluorescence of GeV. The variation of the emission intensity I as a function of the angle θ is shown in Figs. 5(c) and 5(d). We fit the data using the equation $I = \alpha + \beta \sin^2(\theta + \phi)$, where α, β, and ϕ are the fitting parameters. Inferred from the figures, we deduced that each center possesses a preferred single linear polarization. The visibility or the degree of polarization calculated by $V = I_{max} - I_{min}/I_{max} + I_{min}$ is found to be around 92%. This high polarization visibility makes these GeV centers potential candidates for single photon source applications and for quantum key distribution (QKD) applications, which require photons with a well-defined polarization state.

IV. CONCLUSION

In this article, we show that single GeV$^-$ centers in very small NDs grown by HPHT display superior optical properties at room temperature as compared to their bulk counterpart. Assuming that our emitters follow an extended three level system with intensity dependent de-shelving, we developed a model and optimized its parameters to fit the experimental data. The model was validated on several GeVs at different excitation powers. We have studied the single photon emission properties of the GeV centers and their internal population dynamics represented by rate coefficients. We have also characterized their brightness, lifetime, and polarization. The brightest GeV$^-$ studied had a maximum count rate of 1.6 MHz and acts as a single dipole emitter. As such, GeV$^-$ color centers in such small NDs have demonstrated favorable properties for solid state single photon source applications. In future works, we will focus on studying the indistinguishability of the photons emitted from these GeV centers. In addition, we aim to couple these single GeV centers in NDs to a photonic platform made of an ion exchange glass waveguide, toward the realization of a quantum integrated photonic circuit.[44]

AUTHORS' CONTRIBUTIONS

M.N. carried out the experiments, performed the data acquisition, analyzed the data, and wrote the manuscript. D.A. developed the optimization algorithm for the fitting models and wrote the Matlab codes. R.D. helped in the use of the instrumentation for the micro-PL experimental setup. V.D., L.K., and V.A. provided the GeV nanodiamond samples and performed transmission electron microscopy (TEM) for the nanodiamond samples. C.C. conducted the research project, supervised the work technically, discussed the obtained results, and edited the paper. All authors reviewed the manuscript.

ACKNOWLEDGMENTS

The authors are thankful to the European Commission [European Union's Horizon 2020 Research and Innovation Program under Marie Sklodowska-Curie Grant Agreement No. 765075 (LIMQUET)]. They also thank the platform Nano'Mat (http://www.nanomat.eu) where experiments were carried out. V.D. and L.K. thank the Russian Foundation for Basic Research for financial support (Grant No. 18–03-00936).

The authors declare no conflict of interest.

DATA AVAILABILITY

The data that support the findings of this study are available within the article and its supplementary material.

REFERENCES

[1]I. Aharonovich, S. Castelletto, D. Simpson, C. Su, A. Greentree, and S. Prawer, Rep. Prog. Phys. **74**, 076501 (2011).
[2]T. D. Ladd, F. Jelezko, R. Laflamme, Y. Nakamura, C. Monroe, and J. L. O'Brien, Nature **464**, 45 (2010).
[3]L. Childress, R. Walsworth, and M. Lukin, Phys. Today **67**(10), 38 (2014).
[4]G. Balasubramanian *et al.*, Nat. Mater. **8**, 383 (2009).
[5]M. W. Doherty, N. B. Manson, P. Delaney, F. Jelezko, J. Wrachtrup, and L. C. Hollenberg, Phys. Rep. **528**, 1 (2013).
[6]C. Wang, C. Kurtsiefer, H. Weinfurter, and B. Burchard, J. Phys. B **39**, 37 (2006).
[7]S. Meesala *et al.*, Phys. Rev. B **97**, 205444 (2018).
[8]E. Neu, M. Agio, and C. Becher, Opt. Express **20**, 19956 (2012).
[9]A. Sipahigil *et al.*, Science **354**, 847 (2016).
[10]B. Pingault, D.-D. Jarausch, C. Hepp, L. Klintberg, J. N. Becker, M. Markham, C. Becher, and M. Atatüre, Nat. Commun. **8**, 15579 (2017).
[11]K. D. Jahnke, A. Sipahigil, J. M. Binder, M. W. Doherty, M. Metsch, L. J. Rogers, N. B. Manson, M. D. Lukin, and F. Jelezko, New J. Phys. **17**, 043011 (2015).
[12]D. D. Sukachev, A. Sipahigil, C. T. Nguyen, M. K. Bhaskar, R. E. Evans, F. Jelezko, and M. D. Lukin, Phys. Rev. Lett. **119**, 223602 (2017).
[13]Y.-I. Sohn *et al.*, Nat. Commun. **9**, 2012 (2018).
[14]L. J. Rogers *et al.*, Nat. Commun. **5**, 4739 (2014).
[15]T. M. Babinec, B. J. Hausmann, M. Khan, Y. Zhang, J. R. Maze, P. R. Hemmer, and M. Lončar, Nat. Nanotechnol. **5**, 195 (2010).
[16]D. Englund, B. Shields, K. Rivoire, F. Hatami, J. Vuckovic, H. Park, and M. D. Lukin, Nano Lett. **10**, 3922 (2010).
[17]J. Benedikter *et al.*, Phys. Rev. Appl. **7**, 024031 (2017).
[18]H. Siampour, S. Kumar, V. A. Davydov, L. F. Kulikova, V. N. Agafonov, and S. I. Bozhevolnyi, Light **7**, 61 (2018).
[19]K. G. Fehler, A. P. Ovvyan, L. Antoniuk, N. Lettner, N. Gruhler, V. A. Davydov, V. N. Agafonov, W. H. Pernice, and A. Kubanek, Nanophotonics **9**, 3655 (2020).
[20]E. Neu, D. Steinmetz, J. Riedrich-Möller, S. Gsell, M. Fischer, M. Schreck, and C. Becher, New J. Phys. **13**, 025012 (2011).
[21]E. Neu, F. Guldner, C. Arend, Y. Liang, S. Ghodbane, H. Sternschulte, D. Steinmüller-Nethl, A. Krueger, and C. Becher, J. Appl. Phys. **113**, 203507 (2013).
[22]S. Choi, V. Leong, V. A. Davydov, V. N. Agafonov, M. W. Cheong, D. A. Kalashnikov, and L. A. Krivitsky, Sci. Rep. **8**, 3792 (2018).
[23]S. Lindner *et al.*, New J. Phys. **20**, 115002 (2018).
[24]M. K. Bhaskar *et al.*, Phys. Rev. Lett. **118**, 223603 (2017).
[25]J. Goss, P. Briddon, M. Rayson, S. Sque, and R. Jones, Phys. Rev. B **72**, 035214 (2005).
[26]T. Iwasaki *et al.*, Sci. Rep. **5**, 12882 (2015).
[27]Y. N. Palyanov, I. N. Kupriyanov, Y. M. Borzdov, and N. V. Surovtsev, Sci. Rep. **5**, 14789 (2015).
[28]T. Iwasaki, Y. Miyamoto, T. Taniguchi, P. Siyushev, M. H. Metsch, F. Jelezko, and M. Hatano, Phys. Rev. Lett. **119**, 253601 (2017).
[29]S. D. Tchernij *et al.*, ACS Photonics **4**, 2580 (2017).
[30]S. Ditalia Tchernij *et al.*, ACS Photonics **5**, 4864 (2018).
[31]M. E. Trusheim *et al.*, Phys. Rev. B **99**, 075430 (2019).
[32]E. Ekimov, V. Krivobok, S. Lyapin, P. Sherin, V. Gavva, and M. Kondrin, Phys. Rev. B **95**, 094113 (2017).
[33]J. Walker, Rep. Prog. Phys. **42**, 1605 (1979).
[34]G. Davies, Rep. Prog. Phys. **44**, 787 (1981).
[35]S. Häußler *et al.*, New J. Phys. **19**, 063036 (2017).
[36]E. Neu *et al.*, Appl. Phys. Lett. **98**, 243107 (2011).
[37]L. J. Rogers *et al.*, Phys. Rev. Appl. **11**, 024073 (2019).
[38]C. Kurtsiefer, S. Mayer, P. Zarda, and H. Weinfurter, Phys. Rev. Lett. **85**, 290 (2000).

[39]C. Wang, "A solid-state single photon source based on color centers in diamond," Ph.D. thesis (LMU, 2007).
[40]F. Treussart, A. Clouqueur, C. Grossman, and J.-F. Roch, Opt. Lett. **26**, 1504 (2001).
[41]E. Wu, V. Jacques, H. Zeng, P. Grangier, F. Treussart, and J.-F. Roch, Opt. Express **14**, 1296 (2006).
[42]G. Thiering and A. Gali, Phys. Rev. X **8**, 021063 (2018).
[43]A. Beveratos, R. Brouri, T. Gacoin, J.-P. Poizat, and P. Grangier, Phys. Rev. A **64**, 061802 (2001).
[44]X. Xu *et al.*, Photonics Res. **8**, 1541 (2020).
[45]See supplementary material at https://www.scitation.org/doi/suppl/10.1116/5.0035937 for the details growth technique, experimental setup used for optical characterization, the average and standard deviation of the parameters of the six similar GeVs, and the details on the optimization algorithm and calculations of the parameters.